

## An improvement of the low ionosphere model in comparison with the International Reference Ionosphere (IRI) and other empirical models

*N. V. Smirnova, O. F. Ogloblina, V. A. Vlaskov,  
P. I. Vellinov\**

*Polar Geophysical Institute, USSR Academy of Sciences, Murmansk  
\*Solar-Terrestrial Research Laboratory, Bulgarian Academy  
of Sciences, Sofia*

### Introduction

For the improvement of forecast methods in radiowave propagation and practical support of radiocommunications, it is necessary to know the distribution of the basic parameters, determining the character of radiodiffusion and, above all, to have an adequate model for electron concentration distribution in the low ionosphere (50-100 km). In spite of the numerous direct (*in situ*) and indirect experiments on the structure and composition of that region, there are no satisfactory photochemical models yet, complying with the experimental data. The process of low ionosphere modelling is mainly two-directional:

1. Empirical modelling on the basis of systematization, classification of experimental data and working out the dependency of the main ionosphere parameter — the electron concentration  $N$  from all factors, influencing the character of the  $N(h)$ -profile. Examples of such models are the International Reference Ionosphere (IRI) [7], the statistical model of McNamara [8], and the empirical model, created recently at the Scientific Research Institute of Radiophysics (NIRFI)-Gorki, USSR [1]. All above mentioned empirical models of electron density profiles  $N(h)$  require the following initial parameters: date, month, year, local time LT, solar zenith angle  $X$ , latitude, solar activity ( $R$ ,  $F_{10.7}$ ) and magnetic activity ( $K_p$ ,  $A_p$ ).

2. Theoretical modelling where the electron concentration is calculated by the ionization-recombination cycle of the D-region, including the ionization processes; the system of chemical processes of the ion transformation and the recombination processes. The quality of these models and their ability to reproduce the real conditions, observed in the ionosphere, are tested by a

comparison with the experimental data. The simplified models [9, 10], the detail models [11, 12, 13] and the ionization-recombination cycle model developed by us [2, 3, 14, 15] fall in that type of models.

### Theoretical model of the low ionosphere

Our model (Fig. 1) includes: four positive ions —  $\text{NO}^+$ ,  $\text{O}_2^+$ ,  $\text{Cl}_1^+$  and  $\text{Cl}_2^+$ ; four negative ions —  $\text{O}_2^-$ ,  $\text{O}^-$ ,  $\text{CO}_3^-$  and  $\text{NO}_3^-$  and electrons. The rate constants of the major processes in the scheme are presented in Table 1. A detailed reasoning of the model is given in [2, 3, 14]. Herewith, we shall mention only the peculiarities of our model differentiating it from the theoretical models developed earlier. The rates of the transformation processes of the primary positive ions  $\text{NO}^+$ ,  $\text{O}_2^+$  in cluster ions  $\text{Cl}_1^+$ ; of the simpler cluster ions  $\text{Cl}_1^+$  into most complex ones  $\text{Cl}_2^+$ , as well as of primary negative ions  $\text{O}_2^-$  and  $\text{O}^-$  into the intermediate ion  $\text{CO}_3^-$  are illustrated by the effective parameters  $B_{\text{O}_2^+}$ ,  $B_{\text{NO}^+}$ ,  $\beta$ ,  $B_{\text{O}_2^-}$ ,  $B_{\text{O}^-}$ . These effective parameters are deduced from the detailed schemes of ion transformation and include dependencies on the atmospheric temperature  $T$  and humidity [ $\text{H}_2\text{O}$ ], as well as from the small neutral constituents  $\text{O}$ ,  $\text{O}_3$  and  $\text{CO}_2$  concentration.

For example, the rate  $B_{\text{NO}^+}$  of the basic channel of formation of  $\text{Cl}_1^+$  from  $\text{NO}^+$  under normal and winter anomaly conditions has a temperature dependency  $T^{-14}$  in the range  $T=120 \div 230$  K and a greater degree of dependency  $T^{-20,4}$  in the range  $180 \div 240$  K, while under sufficiently high temperature conditions (i. e. in winter) it depends on the humidity of the atmosphere. Under disturbed conditions (auroral absorption AA, polar cap absorption PCA, post-storm effects PSE after magnetic storms SSC) the rate of  $B_{\text{O}_2^+}$  of the basic channel of formation of  $\text{Cl}_1^+$  from  $\text{O}_2^+$  depends on the concentration of  $\text{O}$  and  $\text{H}_2\text{O}$  under all temperature conditions and has a weaker temperature dependency  $T^{-4,4}$ . The same temperature dependency is characteristic of the transformation rate  $\beta$  of the cluster ions  $\text{Cl}_1^+$  with recombination coefficient  $\alpha(\text{Cl}_1^+) = 2 \cdot 10^{-6} \text{ cm}^3 \cdot \text{s}^{-1}$  into more complex cluster ions  $\text{Cl}_2^+$  with recombination coefficient  $\alpha(\text{Cl}_2^+) = 10^{-5} \text{ cm}^3 \cdot \text{s}^{-1}$ .

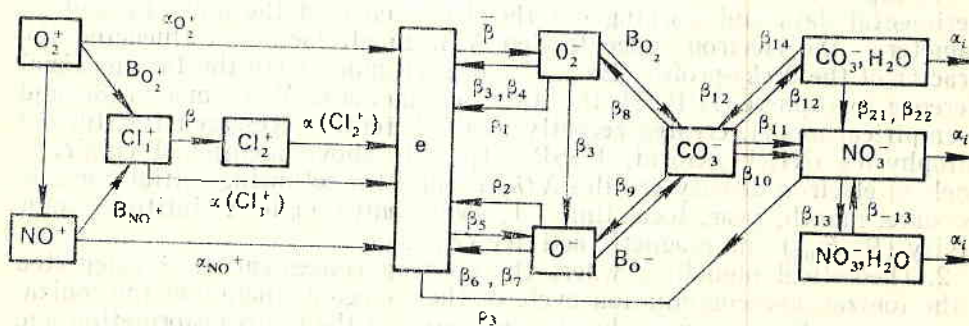


Fig. 1. The proposed theoretical ionization-recombination cycle model of the D-region



Table 1

Rate constant	Rate constant
$\beta_1 = 1,4 \cdot 10^{-29} \left(\frac{300}{T}\right) \exp\left(-\frac{600}{T}\right)$	$\beta_{13} = 7,5 \cdot 10^{-29} \left(\frac{300}{T}\right)^{13}$
$\beta_2 = 1,0 \cdot 10^{-31}$	$\beta_{13} = 5,4 \cdot 10^{-4} \left(\frac{300}{T}\right)^{14} \exp\left(-\frac{7350}{T}\right)$
$\beta_3 = 1,5 \cdot 10^{-10}$	$\beta_{14} = 1,2$
$\beta_4 = 2,0 \cdot 10^{-10}$	$\beta_{15} = 4,0 \cdot 10^{-31} \left(\frac{300}{T}\right)^5$
$\beta_5 = 9,1 \cdot 10^{-13} \left(\frac{300}{T}\right)^{-1,46}$	$\beta_{16} = 2,0 \cdot 10^{-29} \left(\frac{300}{T}\right)^5$
$\beta_6 = 1,9 \cdot 10^{-10}$	$\beta_{17} = 6,0 \cdot 10^{-10}$
$\beta_7 = 2,0 \cdot 10^{-10}$	$\beta_{18} = 9,0 \cdot 10^{-31} \left(\frac{300}{T}\right)^5$
$\beta_8 = 1,1 \cdot 10^{-10}$	$\beta_{19} = 3,1 \cdot 10^{-28} \left(\frac{300}{T}\right)^5$
$\beta_9 = 0,15$	$\beta_{20} = 5,3 \cdot 10^{-10}$
$\beta_{10} = 1,1 \cdot 10^{-11}$	$\beta_{21} = 7,0 \cdot 10^{-12}$
$\beta_{11} = 2,0 \cdot 10^{-10}$	$\beta_{22} = 1,5 \cdot 10^{-10}$
$\beta_{12} = 1,0 \cdot 10^{-28} \left(\frac{300}{T}\right)^{13}$	$\rho_1 = 0,33$
$\beta_{-12} = 7,95 \cdot 10^{-4} \left(\frac{300}{T}\right)^{14} \exp\left(-\frac{7100}{T}\right)$	$\rho_2 = 1,4$
	$\alpha_l = 6,8 \cdot 10^{-7} T^{-0,4}$

$$\text{BO}_2^- = \beta_{15} [\text{O}_2]^2 + \beta_{16} [\text{CO}_2] [\text{O}_2] + \beta_{17} [\text{O}_3]$$

$$\text{BO}^- = \beta_{18} [\text{O}_2]^2 + \beta_{19} [\text{CO}_2] [\text{O}_2] + \beta_{20} [\text{O}_3]$$

Unlike the empirical models, our theoretical model requires the following input parameters: the neutral atmosphere model ( $T_n$ ,  $M_n$ ); the small neutral constituents NO, H<sub>2</sub>O, O<sub>3</sub>, O, O<sub>2</sub> ( $\Delta g$ ) model; the solar radiation intensity model in some lines and ranges of the wavelength; a corpuscule ionization source model, especially when the high-latitude ionosphere is considered. Also, it is necessary for these parameters to depend on the input parameters, as it is with the empirical models: date,  $L$ ,  $T$ ,  $X$ ,  $\theta$ ,  $R$ ,  $F_{10,7}$ ,  $K_p$ ,  $A_p$ . All input parameters of our model are given in [4].

Accuracy of the  $N(h)$ -profiles description on the basis of the theoretical and empirical models

Now we shall evaluate the possibilities of the empirical models [1, 7, 8] and our theoretical model [2-4, 14, 15] so as to render the experimental data  $N$  in the D-region under different heliophysical conditions. For that purpose we are going to use the data bank of NIRFI [1]. In that bank more than 500 electron density profiles are included for a 60-90 km height with 5 km altitude step for the middle latitudes under day conditions.

These data is obtained using different methods: cross-modulation, partial reflection, rocket measurements, etc. As a criterion for the precision of the different models we are defining the reduced logarithmic total error

$$\bar{D} = \frac{1}{n} \sum_{i=1}^n |\ln N_{\text{ex}}/N_{\text{m}}|_i,$$

where  $N$  is the electron concentration,  $n$  is the number of the compared data in the bank; the index "ex" denotes an experimental value, and "m" — model value.

Before considering the results, we shall note that according to the review [16], where a comparative precision of the  $N$  measurement through a number of methods is given, the value of the electron concentration is fixed with precision to the factor from 0,5 to 3. Furthermore, the data concerning the 60-65 km altitudinal interval are given with the lowest precision. That is why, if the data are collected under different heliophysical conditions, it is difficult to expect their representation by the models, with a precision greater than that factor (and, above all, at low altitudes).

The  $D$  values, calculated using the IRI [7], M c N a m a r a [8], NIRFI [1] and our theoretical models for the whole bulk of data set [1], are presented in Table 2.

Table 2

Model	Height, km						
	60	65	70	75	80	85	90
[7]	2,03	0,89	0,747	0,698	0,758	1,04	1,05
[8]	0,722	0,586	0,617	0,602	0,728	0,884	0,899
[1]	1,18	0,775	0,654	0,836	0,923	1,22	1,24
[4,15]	0,926	0,849	0,674	0,680	0,736	0,834	0,845
Case number	107	167	289	405	468	350	266

It can be noted, that on the whole our model describes the data bank better than the empirical models. A certain preference can be given to the model of McNamara for the 60-65 km altitudes. The higher precision of description of the data on these altitudes is explained by the fact that McNamara's model is built up on the basis of a great amount of cross-modulation data — at 60 km they represent about half of the total amount of data, and the values of  $N$  are considerably greater, as compared to the other methods. The chosen values of  $D$  using different methods of measurement show that, if we consider only rocket data (accepted by the COSPAR Symposium on Structure and Methods of Low Ionosphere Measurements — 1973 as most precise and reliable), our model describes experimental data better than the other models [1, 7, 8] for all altitudes, including that at 60-65 km altitude.

Up to now we have considered the possibilities of the models to reproduce  $N$  for the whole data bank, (the profiles are collected in the quiet D-region). Now we are going to present the results obtained by low ionosphere disturbances modelling.

Let us consider several cases of different type: polar cap absorption (PCA), post-storm effects (PSE) and winter anomaly (WA). The chosen cases have input parameters necessary for calculation as follows: data for the particle fluxes and their respective electron production rates (PCA, PSE); data for NO and the temperature  $T$  (WA). In Fig. 2 the results from the calculation of 9 cases of PCA (proton flares on August 4th-5th, 1972; November 2nd-4th,



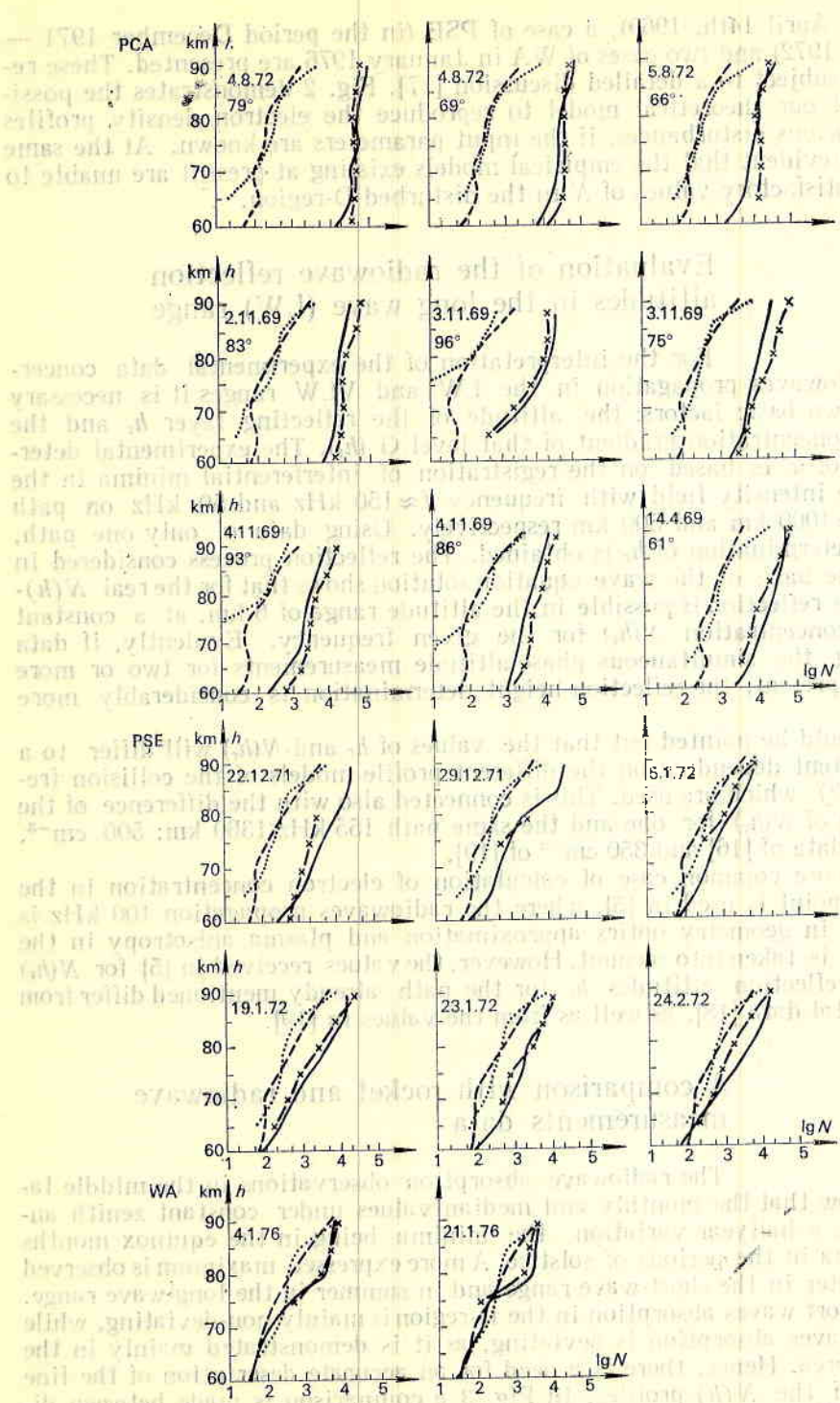


Fig. 2.  $N(h)$ -profiles under different ionospheric disturbances  
 PCA — polar cap absorption; PSE — post-storm effects; WA — winter anomaly;  
 ... IRI [7]; --- [8]; — our theoretical model; ×—× NIRFI [1]

1969 and April 14th, 1969), a case of PSE (in the period December 1971 — February 1972) and two cases of WA in January 1976 are presented. These results are subject to a detailed discussion [17]. Fig. 2 demonstrates the possibilities of our theoretical model to reproduce the electron density profiles during various disturbances, if the input parameters are known. At the same time it is evident that the empirical models existing at present are unable to present satisfactory values of  $N$  in the disturbed D-region.

### Evaluation of the radiowave reflection altitudes in the long wave (LW) range

For the interpretation of the experimental data concerning radiowaves propagation in the LW and VLW ranges it is necessary to know two basic factors: the altitude of the reflecting layer  $h_r$  and the electron concentration gradient of that level  $G(h_r)$ . The experimental determination of  $h_r$  is based on the registration of interferential minima in the radiowave intensity field with frequency  $f \approx 150$  kHz and 50 kHz on path length  $l \approx 1000$  km and 500 km respectively. Using data of only one path, a rough determination of  $h_r$  is obtained. The reflection process considered in [16] on the basis of the wave equation solution shows that for the real  $N(h)$ -profiles the reflection is possible in the altitude range of 6 km, at a constant electron concentration  $N(h_r)$  for the given frequency. Evidently, if data concerning the simultaneous phase-altitude measurements for two or more paths are present, the reflection height determination is considerably more precise.

It should be pointed out that the values of  $h_r$  and  $N(h_r)$  will differ to a certain extent depending on the different profile models of the collision frequency  $\nu(h)$  which are used. This is connected also with the difference of the evaluation of  $N(h_r)$  for one and the same path 155 kHz/1360 km:  $500 \text{ cm}^{-3}$ , following data of [16] and  $350 \text{ cm}^{-3}$  of [19].

The more common case of calculation of electron concentration in the reflection point is used in [5], where the radiowaves propagation 100 kHz is considered in geometry optics approximation and plasma anisotropy in the ionosphere is taken into account. However, the values received in [5] for  $N(h_r)$  and the reflection altitudes  $h_r$  for the path already mentioned differ from experimental data [18], as well as from the values in [19].

### A comparison with rocket and radiowave measurements data

The radiowave absorption observations in the middle latitudes show that the monthly and median values under constant zenith angle  $X$  have a half-year variation, the minima being in the equinox months and maxima in the periods of solstice. A more expressed maximum is observed during winter in the short-wave range and in summer in the long-wave range.

The short waves absorption in the D-region is mainly non-deviating, while the long waves absorption is deviating, as it is demonstrated mainly in the reflection area. Hence, there is a need for an accurate description of the fine structure of the  $N(h)$ -profiles. In Fig. 3 a comparison is made between different profile models: the  $N(h)$ -distribution according to our theoretical model of the D-region, the rocket profile measured in the Volgograd ( $47^\circ \text{ N}$ ,



April,  $X=80^\circ$ , low solar activity) [6] and the profiles calculated according to the models of IRI [1], and Bremer and Singer [20]. Herewith, the altitude of radiowave reflection is also shown as obtained by means of the phase-altitude method via the simultaneous two-path long-wave experiment of 218 kHz/1463 km and 191 kHz/1278 km, with reflection point around Volgograd [6]. The reflection altitude corresponds to an electron concentration about  $550 \text{ cm}^{-3}$ .

It is evident that the theoretical model describes most precisely the experimental *in situ*  $N(h)$ -profile and much better than the other models corresponds to the results from the phase-altitude measurements.

An adequately precise evaluation of the radiowave reflection altitude in the long-wave range on the basis of our model is corroborated by the comparison between the  $h_r$  calculated for the Allouis (France) — Sofia ( $f_i=26 \text{ kHz}$ ) path and the results of the phase-altitude measurements for the Brashov-Kühlungsborn 155 kHz/1360 km ( $f_i=26 \text{ kHz}$ ). For example, for April, at a low solar activity our theoretical model gives (for  $X=78^\circ$  and  $68^\circ$ ) reflection altitudes of 76.5 and 74 km, as compared to the experimental data of 78 and 75.5 km respectively.

### Conclusion

Thus, the different tests of our theoretical model of the low ionosphere carried out on the basis of a major experimental dataset shows that our model allows considerably more precise reproduction of the experimental data according to the basic ionospheric characteristic, the  $N(h)$ -profiles, as well as to obtaining a better correspondence with them, as compared to the existing empirical models of IRI [7], Mc Namara [8], NIRFI [1] and others. Besides this, the advantages of our model as compared to the empirical models are proved both for indirect data concerning radiowave propagation and for the *in situ* rocket measurements. It is valid for quiet conditions (Fig. 3) and to a great extent for the different types of disturbed conditions (Fig. 2) in the solar-terrestrial relationships of ionospheric (PCA), magnetospheric (PSE) and meteorological (WA) character.

The advantages of our model (Fig. 1) are in the sufficiently correct calculation of the existing in the mesosphere diurnal, seasonal and 11-year variations of the temperature, humidity and concentration of the minor neutral constituents.

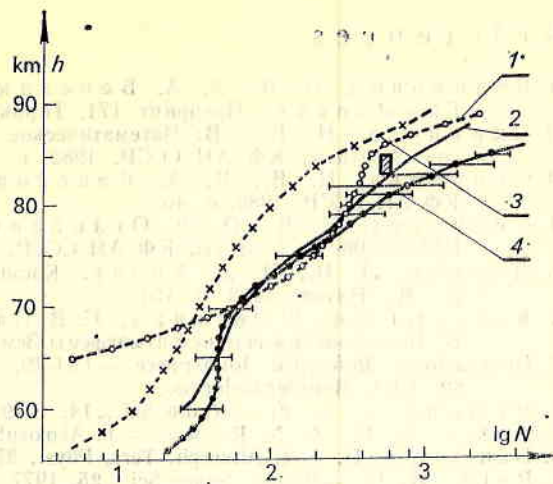


Fig. 3. A comparison between  $N(h)$ -profiles calculated following the IRI-79 model [7] (1), the theoretical model [2-4, 14, 15] (2), the experimental data model [20] (3); (4) rocket measurements [6], the phase-altitudinal method [6] — hatching

## References

1. Беликович, В. В., Е. А. Бенедиктов, В. Д. Вяхирев, Л. В. Гришквич. Препринт 171. Горький, НИРФИ, 1983, с. 51.
2. Смирнова, Н. В. — В: Математическое моделирование комплексных процессов. Апатиты, КФ АН СССР, 1982, с. 22.
3. Смирнова, Н. В., В. А. Власков. Препринт ПГИ 82-3-17. Апатиты, КФ АН СССР, 1982, с. 46.
4. Смирнова, Н. В., О. Ф. Оглоблина, В. А. Власков. Препринт ПГИ 84-08-36. Апатиты, КФ АН СССР, 1984, с. 31.
5. Дорман, Л. И., И. Д. Козин. Космическое излучение в верхней атмосфере. М., Наука, 1983, с. 151.
6. Косарт, Г. фон, Г. Энтзиан, С. В. Пахомов, Д. А. Тарасенко. — В: Исследования верхней атмосферы Земли. М., Гидрометеоиздат, 1984, с. 191.
7. International Reference Ionosphere — IRI-79, World Data Center A, Report UAG-82, 1981, Boulder/Colorado.
8. McNamara, L. F. — Radio Sci., 14, 1979, No 6, p. 1165.
9. Mitra, A. P., J. N. Rowe. — J. Atmosph. Terr. Phys., 34, 1972, No 5, p. 795.
10. Danilov, A. D. — J. Atmosph. Terr. Phys., 37, 1975, No 6/7, p. 885.
11. Reid, G. C. — Planet. Space Sci., 25, 1977, p. 275.
12. Chakrabarty, D. K., P. Chakrabarty, G. Witt. — J. Atmosph. Terr. Phys., 40, 1978, No 4, p. 437.
13. Torcar, K. M., Friedrich. — J. Atmosph. Terr. Phys., 45, 1983, No 6, p. 369.
14. Vellinov, P. I., N. A. Smirnova, V. A. Vlasikov. — Adv. Space Res., 4, 1984, No 1, p. 123.
15. Vellinov, P. I., N. A. Smirnova, N. A. Vlasikov. — Handbook for MAP (Ed. by SCOSTEP/NASA, Univ. of Illinois, Urbana), 10, 1984, p. 70.
16. Thrane, E. V. — In: Methods of Measurements and Results of Lower Ionosphere Structure, Berlin, Akademie Verlag, 1974, p. 3.
17. Vellinov, P. I., V. A. Vlasikov, N. V. Smirnova, O. F. Ogloblina, Chr. W. Spassov. — Аерокосмически изследвания в България, 7, 1991, с. 11.
18. Lauter, E. A., J. Taubenheim, G. Entzian et al. — HIM-STR-Report, 7, 1976, p. 83.
19. Bremer, J., K. Evers, J. Taubenheim. — Gerlands Beitr. Geophys./90, 1981, No 4, p. 296.
20. Bremer, J., W. Singer. — J. Atmosph. Terr. Phys., 39, 1977, No 1, p. 25.
21. Cossart, G. von, S. V. Pakhomov. — Handbook for MAP (Ed. by SCOSTEP/NASA, Univ. of Illinois, Urbana), 10, 1984, p. 34.

Одно улучшение модели нижней ионосферы по сравнению с международной справочной ионосферой (IRI) и с другими эмпирическими моделями

*Н. В. Смирнова, О. Ф. Оглоблина, В. А. Власков,  
П. И. Велинов*

(Резюме)

Предлагается теоретическая модель нижней ионосферы, включающей четыре положительных иона ( $O^+$ ,  $O_2^+$ ,  $Cl_1^+$ ,  $Cl_2^+$ ), четыре отрицательных иона и электроны. Она учитывает зависимость скоростей основных процессов от температуры, влажности атмосферы и концентрации малых нейтральных составляющих. Проверка разработанной теоретической модели на большом массиве экспериментальных данных (свыше 1000  $N(h)$ -профилей) показывает, что она лучше воспроизводит эмпирические модели, чем известные сезонные и суточные вариации  $N(h)$ , а также профили во время различных ионосферных возмущений.